Long-time tracer diffusion of nonspherical Brownian particles

F. de J. Guevara-Rodríguez
Coordinación de Simulación Molecular, Instituto Mexicano del Petróleo, Eje Lázaro Cárdenas 152, 07730, Distrito Federal, México

M. Medina-Noyola
Instituto de Física ''Manuel Sandoval Vallarta,'' Universidad Autónoma de San Luis Potosí, Alvaro Obregón 64, 78000, San Luis Potosí, SLP, México

(Received 7 December 1999)

The long-time tracer-diffusion properties of a nonspherical Brownian particle that interacts with a suspension of spherical particles are studied in terms of an idealized but nontrivial two-dimensional model system. For this system, the predictions of the generalized Langevin equation approach to tracer diffusion can be calculated, and compared with the (extrapolated) results of a computer simulation experiment. In the model, the nonspherical particle is represented by a rigid linear array of N_T (=2 or 3) spherical particles with nearest-neighbor separation ΔL. We calculate the long-time rotational and (transverse and longitudinal) translational diffusion coefficients. The theory is found to reproduce qualitatively and quantitatively the main features of the extrapolated results. Finally, we also present theoretical results that derive from still simpler approximate theoretical schemes.

PACS number(s): 05.20.−y

I. INTRODUCTION

The diffusion properties of suspensions of *spherical* colloidal particles have been the subject of considerable interest for many years [1–5]. In fact, there are some theoretical methods aimed at explaining the main features of these dynamic properties in terms of interparticle forces [2–5]. However, the statistical mechanical description of the diffusion properties of suspensions involving *nonspherical* particles is still to be developed. Recently, however, one such method, namely, the generalized Langevin equation (GLE) approach to tracer diffusion [5] has been extended [6] to study the Brownian motion of a suspension with nonspherical particles. In this paper, we present the predictions of this theoretical approach as applied to the description of the diffusion properties of nonspherical colloidal tracer particles. The nonspherical Brownian particle of our model system is represented by a linear array of N_T (=2 or 3) spherical particles with nearest-neighbor separation ΔL, rigidly bound to each other by imaginary forces. This nonspherical particle executes Brownian motion while interacting with the Brownian particles of the supporting two-dimensional colloidal suspension only through direct interactions (i.e., in the absence of hydrodynamic interactions). Here we report some aspects of our study of tracer-diffusion phenomena in this simple but not trivial model system. We study the dependence of the long-time rotational and traslational diffusion coefficients of the nonspherical particle on parameters such as the particle concentration n of the supporting suspension. Our aim is only to describe a few general features of these long-time properties, and to assess the accuracy of the predictions of the GLE approach, by means of their comparison with the results of a computer simulation experiment.

In the following section we provide a detailed definition of our model system, and summarize the theoretical basis of the approximate theoretical calculation of its time-dependent tracer-diffusion properties in the long-time regime. We report and analyze these theoretical results in the context of their comparison with the calculation of the same properties computed through an extrapolation procedure applied to the Brownian dynamics simulation data of the model. In Sec. III we present and analyze the results of the application of the GLE approach together two approximations, namely, the total and partial superposition approximations. Finally, Sec. IV contains a brief summary of the most relevant conclusions.

II. ANALYSIS OF THE LONG-TIME REGIME

A. Generalized Langevin equation approach

Our system consists of a two-dimensional model Brownian fluid of spherical particles that interact through the hard-sphere plus repulsive Yukawa pair potential

$$\beta u(r)=\begin{cases} K\exp[-z(r/\sigma-1)]/(r/\sigma), & r>\sigma \\ +\infty, & r\leq\sigma, \end{cases} \tag{2.1}$$

where σ is the hard-sphere diameter, $\beta^{-1}=k_BT$, with k_B being Boltzmann's constant and T the temperature, z is the screening parameter (in units of σ^{-1}), and K is the potential energy of two particles at contact, in units of k_BT. These spherical (i.e., circular or disklike in our two-dimensional system) particles are present at bulk number concentration n (or reduced number concentration $n^*\equiv n\sigma^2$). In addition to these spherical Brownian particles, we also have a single *nonspherical* Brownian particle, namely, a rigid linear array of N_T spherical particles, whose interaction with one of the ''free'' spheres located at position $\mathbf{r}$ is given by

$$\psi(\mathbf{r})=\sum_{i=1}^{N_T} u(|\mathbf{r}-\mathbf{R}_i|), \tag{2.2}$$

where $\mathbf{R}_i$ $(i=1,2,\ldots,N_T)$ are the positions of the N_T spheres that constitute the nonspherical particle. In the reference frame attached to this rigid array, each one of the $\mathbf{R}_i$

remains constant and is chosen to lie along the Y axis, so that its Cartesian coordinates are $X_i=0$ and $Y_i=(N_T+1-2i)\Delta L/2$. In this paper we consider only two cases, namely, a ''dimer'' ($N_T=2$) and a ''trimer'' ($N_T=3$). Furthermore, throughout this work we shall keep the values of the Yukawa parameters fixed to $K=500$ and $z=0.15$, which correspond to a system and conditions widely studied elsewhere in the absence of the nonspherical tracer particle [7].

The purpose of this work is to present results for the long-time translational and rotational diffusion coefficients, defined as

$$D_\alpha^L=\lim_{t\to\infty}\frac{\langle[\Delta r_\alpha(t)]^2\rangle}{2t},\quad \alpha=\perp,\parallel,R, \tag{2.3}$$

where $\Delta r_\perp(t)$ and $\Delta r_\parallel(t)$ are, respectively, the components of the translational displacement of the tracer particle's center of mass at time t in the transverse ($\perp$) and longitudinal ($\parallel$) directions refered to the particle's main axis, whereas $\Delta r_R(t)$ is the angular displacement at time t. The long-time diffusion coefficients contain information on the effects of direct interactions between the tracer particle and all the spherical particles around it. On the other hand, these diffusion coefficients are related to the friction coefficients by Einstein's relation,

$$D_\alpha^L=\frac{k_BT}{\xi_\alpha^0+\Delta\xi_\alpha}, \tag{2.4}$$

where ξ_α^0 is the free-diffusion friction coefficient (i.e., in the absence of interactions), whereas $\Delta\xi_\alpha$ represents the contribution of the direct interactions to the total effective friction on the tracer. This term $\Delta\xi_\alpha$ in Eq. (2.4) is the time integral of the time-dependent friction function $\Delta\xi_\alpha(t)$. The main result of the generalized Langevin equation approach [5] is a general expression for this property. For our model system, an approximate form of such a general expression, on which we will base our present work, is

$$\Delta\xi_\alpha=\int_0^\infty dt\,\Delta\xi_\alpha(t)=\frac{k_BTn}{(2\pi)^2}\int d^2k\frac{|\tilde K_{\mathbf{k}}^{(\alpha)}H(\mathbf{k})|^2}{k^2[S(k)D_{\rm CM}^0+D^0]}. \tag{2.5}$$

In this expression, $S(k)$ is the structure factor of the colloidal fluid in the absence of the nonspherical tracer. The function $H(\mathbf{k})$ is the Fourier transform of the total correlation function $H(\mathbf{r})$ between the tracer and a sphere of the fluid, i.e., $H(\mathbf{r})\equiv G(\mathbf{r})-1$, where $n^{eq}(\mathbf{r})\equiv nG(\mathbf{r})$ is the local concentration of the spheres at position $\mathbf{r}$ around the tracer particle. The operators $\tilde K_{\mathbf{k}}^{(\alpha)}$ are defined by

$$\tilde K_{\mathbf{k}}^{(\perp)}\equiv -ik_x,\quad \tilde K_{\mathbf{k}}^{(\parallel)}\equiv -ik_y,\quad \tilde K_{\mathbf{k}}^{(R)}\equiv k_x\frac{\partial}{\partial k_y}-k_y\frac{\partial}{\partial k_x}. \tag{2.6}$$

In this paper, we focus on the application of this expression for the friction function to compute the diffusion coefficients of our nonspherical particle as a function of the concentration n of the spherical particles. The details of the derivation of Eq. (2.5) for $\Delta\xi_\alpha(t)$ are given in previous papers [8,9], from which we adopt all the definitions and concepts. Thus, the parameter $D_{\rm CM}^0\equiv(D_\perp^0+D_\parallel^0)/2$ in Eq. (2.5) is the free-diffusion coefficient of the center of mass of the tracer defined in terms of the perpendicular and parallel diffusion coefficients. As in Refs. [8] and [9], the translational and rotational free-diffusion coefficients of the tracer are assumed to be given by

$$D_\perp^0=D_\parallel^0=D^0/N_T\quad\text{and}\quad D_R^0=D^0/N_T\mathcal{R}^2, \tag{2.7}$$

where $\mathcal{R}$ is the radius of gyration of our nonspherical particle, i.e.,

$$\mathcal{R}^2\equiv\sum_{i=1}^{N_T}r_i^2/N_T, \tag{2.8}$$

with r_i being the distance between the ith sphere of the tracer particle and the tracer's center of mass. The definition of the free-diffusion coefficients given in Eq. (2.7) is in terms of the free-diffusion coefficient D^0 of a free sphere. The specific value of D^0 will not be needed, since this parameter will only be used to define dimensionless quantities. Finally, the free-diffusion coefficients of the tracer (D_α^0) and of the sphere (D^0) are related to the friction coefficients ξ_α^0 and ξ^0, respectively, through the Einstein relations $D_\alpha^0=k_BT/\xi_\alpha^0$ and $D^0=k_BT/\xi^0$.

Additionally, in order to understand the predicted behavior of D_α^L as a function of the concentration n of the supporting suspension, it will be convenient to analyze the coefficients of the expansion of D_α^L in a power series of the concentration. For this purpose, we first derive the expansion of the friction function $\Delta\xi_\alpha$ in Eq. (2.5), i.e.,

$$\frac{\Delta\xi_\alpha}{\xi_\alpha^0}=\left[\frac{\partial}{\partial n}\left(\frac{\Delta\xi_\alpha}{\xi_\alpha^0}\right)\right]_{n=0}n+\left[\frac{1}{2}\frac{\partial^2}{\partial n^2}\left(\frac{\Delta\xi_\alpha}{\xi_\alpha^0}\right)\right]_{n=0}n^2+\cdots, \tag{2.9}$$

where the coefficients of the linear and quadratic terms are given, respectively, by

$$\left[\frac{\partial}{\partial n}\left(\frac{\Delta\xi_\alpha}{\xi_\alpha^0}\right)\right]_{n=0}=\frac{D_\alpha}{(2\pi)^2}\int d^2k\frac{|\tilde K_{\mathbf{k}}^{(\alpha)}H_0(\mathbf{k})|^2}{k^2(D_{\rm CM}+D^0)}, \tag{2.10a}$$

$$\left[\frac{1}{2}\frac{\partial^2}{\partial n^2}\left(\frac{\Delta\xi_\alpha}{\xi_\alpha^0}\right)\right]_{n=0}=\frac{D_\alpha}{(2\pi)^2}\int d^2k\left(\frac{2\,\mathrm{Re}\{[(\tilde K_{\mathbf{k}}^{(\alpha)}H_0(\mathbf{k})]^*[\tilde K_{\mathbf{k}}^{(\alpha)}H_1(\mathbf{k})]\}}{k^2(D_{\rm CM}+D^0)}-\frac{|\tilde K_{\mathbf{k}}^{(\alpha)}H_0(\mathbf{k})|^2D_{\rm CM}h_0(k)}{k^2(D_{\rm CM}+D^0)^2}\right). \tag{2.10b}$$

In the quadratic coefficient, Re[. . .] is the real part of its argument. Both coefficients are derived from Eq. (2.5), in which, at very low concentrations, we approximate the total correlation function by $H(\mathbf{r})\approx H_0(\mathbf{r})+nH_1(\mathbf{r})+\cdots$ and the

structure factor is approximated by $S(k)=1+nh_0(k)$, where $H_0(\mathbf{r})$, $H_1(\mathbf{r})$, and $h_0(r)$ are defined by

$$H_0(\mathbf{r})=e^{-\beta\psi(\mathbf{r})}-1, \tag{2.11a}$$

$$H_1(\mathbf{r})=e^{-\beta\psi(\mathbf{r})}\int d^2r_1(e^{-\beta\psi(\mathbf{r}_1)}-1)(e^{-\beta u(|\mathbf{r}_1-\mathbf{r}|)}-1), \tag{2.11b}$$

and

$$h_0(r)=e^{-\beta u(r)}-1. \tag{2.11c}$$

From Eqs. (2.4), (2.5), and (2.9), the corresponding expansion for the diffusion coefficients D_α^L of the nonspherical tracer can be written as

$$\frac{D_\alpha^L}{D_\alpha^0}=1-\left[\frac{\partial}{\partial n}\left(\frac{\Delta\xi_\alpha}{\xi_\alpha^0}\right)\right]_{n=0}n+\left\{\left[\frac{\partial}{\partial n}\left(\frac{\Delta\xi_\alpha}{\xi_\alpha^0}\right)\right]_{n=0}^2-\left[\frac{1}{2}\frac{\partial^2}{\partial n^2}\left(\frac{\Delta\xi_\alpha}{\xi_\alpha^0}\right)\right]_{n=0}\right\}n^2+\cdots. \tag{2.12}$$

This concludes the summary of the theoretical aspects of the GLE approach that we will need below. Let us now refer to the computer simulation of the model.

B. Computer simulation

From the computer simulation experiment, we can compute the time-dependent diffusion coefficients $D_\alpha(t)\equiv\langle[\Delta r_\alpha(t)]^2\rangle/2t$ of our nonspherical particle in the intermediate-time regime [9]. Of course, we cannot compute the properties of the tracer in the strictly long-time limit. However, in this paper we estimate these properties as an extrapolation of the available computer simulation data for $D_\alpha(t)$. To fit the computer simulation data we use the expression [10]

$$\frac{D_\alpha(t)}{D_\alpha^0}=\frac{D_\alpha^L}{D_\alpha^0}-\left(\frac{D_\alpha^L}{D_\alpha^0}-1\right)\left(\frac{t_0}{t+t_0}\right), \tag{2.13}$$

where D_α^L and t_0 are the fitting parameters to fit the numerical experimental data. The accuracy of Eq. (2.13) as a fitting device is illustrated in Fig. 1. In this figure we present the numerical simulation data and the corresponding fit for the translational and rotational diffusion coefficients of a dimer with a separation between its spheres of $\Delta L=10\sigma$, in a suspension of reduced concentration of spheres $n^*=0.002$. Obviously, the parameter D_α^L fitted in this manner provides an approximate estimate of the true long-time diffusion coefficient of the tracer, which is the most reliable reference we can use to confront our theoretical predictions for the asymptotic long-time coefficients D_α^L.

Here we shall not provide the details of the Brownian dynamics simulation procedure, since they have been reported and described elsewhere [8,9]. Instead, in the following subsection, we proceed directly to the presentation of the extrapolated results and their use in the comparison with the theoretical predictions for D_α^L.

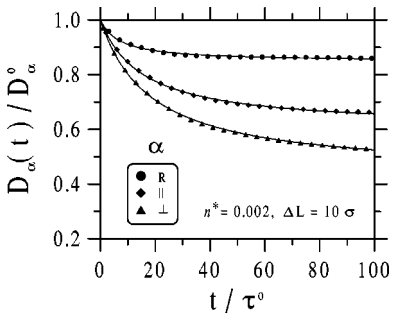

FIG. 1. Ilustration of the time-dependent diffusion coefficients of a dimer ($N_T=2$). Symbols and solid line represent, respectively, the numerical simulation results and its fit. In the figure, $n^*\equiv n\sigma^2$ is the reduced concentration of spheres, and $\tau^0\equiv\sigma^2/D_0$ is the time scale.

C. Comparisons

Before starting with the presentation and discussion of this comparison, it is important to comment on the following. From Eq. (2.5) we can see that one important input of the approximate theory is the total correlation function $H(\mathbf{r})$ between the surrounding spheres and the tracer particle. This function is related to the local concentration $n^{eq}(\mathbf{r})\equiv nG(\mathbf{r})$ of spheres around the tracer by $H(\mathbf{r})=G(\mathbf{r})-1$. At this point, let the local concentration of spheres be computed directly from the computer simulation experiment, so that it represents an *exact* input for the theory. In the same manner, the structure factor $S(k)$ of the homogenous suspension (without the tracer) is also obtained directly from the computer simulation. Thus, the theoretical prediction of the GLE approach will exhibit only the effects of the two main approximations involved in the derivation of Eq. (2.5), namely, the homogeneity approximation and the use of a short-time approximation for the self- and the collective diffusion propagator of the supporting suspension, both of which were discussed in previous publications [8,9].

In Figs. 2 and 3 we present the comparison between the extrapolated and the theoretical results for D_α^L for a dimer ($N_T=2$) and a trimer ($N_T=3$), respectively, as a function of the reduced concentration of surrounding spheres. In both figures, we consider two values of the distance ΔL between nearest-neighbor spheres in the tracer, namely, 10σ and 20σ. In all these figures, the lines are only a guide to the eye, and the symbols indicate the points at which the computer simulation and the theoretical calculations were performed.

As we can see from these figures, the theoretical predictions systematically underestimate the effects of the direct interactions on all the diffusion coefficients. The quantitative disagreement between the theoretical predictions and the simulated results are of the same order as those observed in the application of the same approximation to the calculation of the tracer-diffusion coefficients of *spherical* tracer particles [7]. Here also, the quantitative disagreement exhibited in Figs. 2 and 3 illustrates the extent of the quantitative accuracy of the dynamic approximations involved in the derivation of Eq. (2.5).

The comparison in Figs. 2 and 3, however, also exhibits a complete qualitative agreement between the theoretical calculations and the simulated results, in reference to the functional dependence of $D_\alpha^L(n)$ on the concentration of the sup-

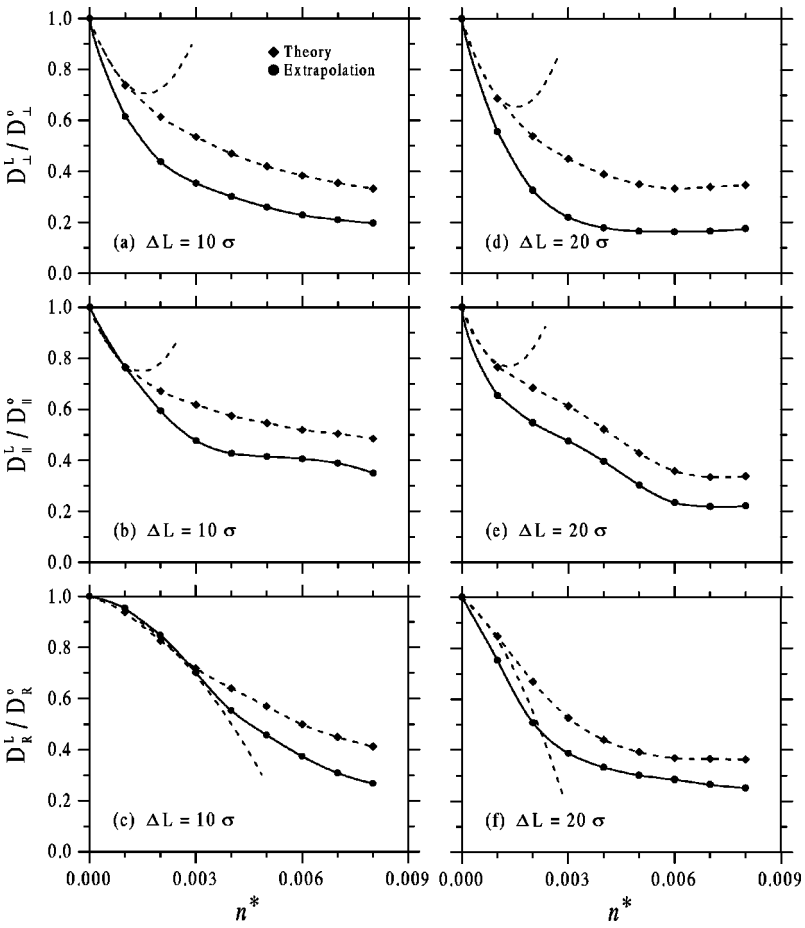

FIG. 2. Comparison between the long-time tracer diffusion coefficients of a dimer ($N_T=2$) computed from the GLE approach (with exact static inputs), and from the extrapolation of the numerical simulation data. Dashed and solid lines are only a guide to the eye. The additional dashed line (without symbols) represents the quadratic expansion in the concentration of the diffusion coefficients.

porting suspension. Among the main features in which we observe full qualitative agreement, we can mention the following. Notice, first, that in all cases, $D_{\perp}^{L}$ and $D_{\parallel}^{L}$ exhibit an upward initial curvature $[(\partial^2 D_{\alpha}^{L}/\partial n^2)_{n=0}>0]$, opposite to what is observes in D_{R}^{L}. To further emphasize this point, we have included in Figs. 2 and 3 the quadratic approximation defined in Eq. (2.12) for the theoretical value of $D_{\alpha}^{L}(n)$ (dashed line without symbols). Notice, also, the changes in curvature in $D_{R}^{L}(n)$ and $D_{\perp}^{L}(n)$ at higher concentrations, which our theoretical results capture generally quite correctly. As illustrated in Figs. 2 and 3, the various cases considered ($D_{\perp}^{L}, D_{\parallel}^{L}, D_{R}^{L}$, for $\Delta L=10\sigma$ and $\Delta L=20\sigma$, and for $N_T=2$ and $N_T=3$) exhibit a much richer dependence on concentration than the fully monotonic dependence always observed in the case of spherical tracer particles. The fact that this qualitative richness is correctly contained in a single expression, such as Eq. (2.5), indicates the usefulness of the GLE approach to derive expressions for dynamic properties in terms solely of the structural information contained in $H(\mathbf{r})$ and $S(k)$.

As we have mentioned before, the theoretical predictions that we have presented here were computed with exact (i.e., simulated) structural inputs, namely, the local concentration of the spheres around the tracer and the radial distribution function of the homogenous fluid. Let us now present the theoretical predictions when we use approximate structural inputs in Eq. (2.5).

III. THE SUPERPOSITION APPROXIMATION

In the previous section, we presented the results of Eq. (2.5) obtained when we used as inputs the exact structural information computed from the simulation experiment. However, this approach has a high computational cost, particularly referring to the computation of the local concentration of spheres $n^{eq}(\mathbf{r})$ around the tracer particle. Thus, a simple form to approximate this function is indeed desirable. Here we consider approximating this distribution function by its superposition approximation [11], as we have done in previous work [12]. The superposition approximation for $n^{eq}(\mathbf{r})$ in the context of our model (in which the spheres that constitute the tracer are of the same type as those of the suspension) can be written as

$$n^{eq}(\mathbf{r}) \approx n \prod_{i=1}^{N_T} g(|\mathbf{r}-\mathbf{R}_i|), \tag{3.1}$$

where $g(r)$ is the radial distribution function of the homogeneous supporting suspension. This radial function is readily provided by the computer experiment at a much lower computational cost. In this section we present the effects of the local concentration $n^{eq}(\mathbf{r})$ being approximated by the superposition approximation, and then employed as the structural input required in the general result of Eq. (2.5).

In addition to the full superposition approximation for $H(\mathbf{k})$ resulting from Eq. (3.1), here we shall also consider a still simpler approximation, which we shall refer to as the *partial* superposition approximation, which is the *exact* value of $H(\mathbf{r})$ in the limit of large spacing ΔL between the spheres that constitute the nonspherical tracer particle. In this limit,

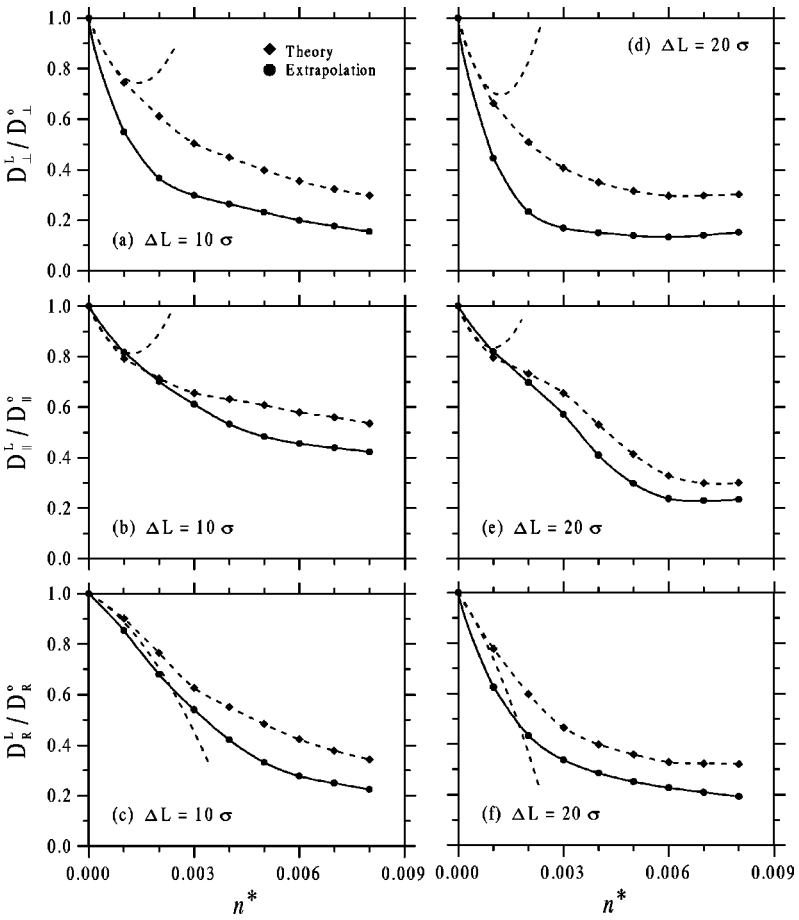

FIG. 3. Same as Fig. 2, but for a trimer ($N_T = 3$).

$$H(\mathbf{r}) \equiv \prod_{i=1}^{N_T} g(|\mathbf{r}-\mathbf{R}_i|) - 1 \approx \sum_{i=1}^{N_T} h(|\mathbf{r}-\mathbf{R}_i|), \qquad (3.2)$$

where $h(r)=g(r)-1$ is the total correlation function of the bulk suspension. Thus, the partial superposition approximation for $H(\mathbf{k})$ can be written as

$$H(\mathbf{k}) \approx \left(\sum_{i=1}^{N_T} \exp(i\mathbf{k}\cdot\mathbf{R}_i) \right) h(k), \qquad (3.3)$$

where $h(k)=[S(k)-1]/n$. This is an approximation that further simplifies the calculation of the integral on $\mathbf{k}$ in Eq. (2.5).

In Figs. 4 and 5 we present a similar comparison as in Figs. 2 and 3, but this time between the simulation results and the theoretical predictions of Eq. (2.5) with the structural property $H(\mathbf{r})$ approximated according to the full superposition approximation [Eq. (3.1)] and to the partial superposition approximation [Eq. (3.3)]. Let us first notice that, in general, both approximations provide quite a reasonable description [i.e., similar to the theoretical results with exact input $H(\mathbf{r})$ as in the previous section] only for the rotational diffusion coefficient D_R^L for both the dimer and the trimer with the longest spacing $\Delta L=20\sigma$ [Figs. 4(f) and 5(f)]. A similar statement could also be made for $D_\perp^L$ [Figs. 4(d) and 5(d)], except that the results of the partial superposition approximation now seems to be slightly more accurate at low concentrations, probably from some form of error cancellation. In fact, this same trend can also be observed for D_R^L and $D_\perp^L$ for the shortest spacing $\Delta L=10\sigma$ for the dimer [Figs. 4(a) and 5(a)] and the trimer [Figs. 5(a) and 5(e)]. In these cases, particularly for D_R^L, we find that the results of the full superposition approximation seem to be quantitatively and even qualitatively less accurate than the results of the partial superposition approximation. Thus, we may conclude that, taking into account the computational simplification of the partial superposition approximation, it seems to provide a more useful approximation to use in a first-order description of D_R^L and $D_\perp^L$ for both the dimer and the trimer, even at the shortest spacing $\Delta L=10\sigma$. In particular, notice that D_R^L obtained for this spacing using the full superposition approximation overestimates rather strongly the effects of the interactions at low concentrations, whereas the results of the partial superposition approximation lie closer to the simulation data, probably due to error cancellation.

The other general observation refers to the rather poor performance of the superposition approximation (both full and partial) in the calculation of $D_\parallel^L$, as illustrated in Figs. 4(b) and 4(e) for the dimer and in Figs. 5(b) and 5(e) for the trimer. In these cases there is not even a pattern that characterizes the accuracy of either of these approximations with regard to the calculation of $D_\parallel^L$. In fact, in contrast to the theoretical results of the previous section, in these cases the theoretical predictions are even qualitatively different from the simulation results.

IV. SUMMARY AND CONCLUSIONS

In this work we have presented computer simulation results for the rotational and translational long-time diffusion

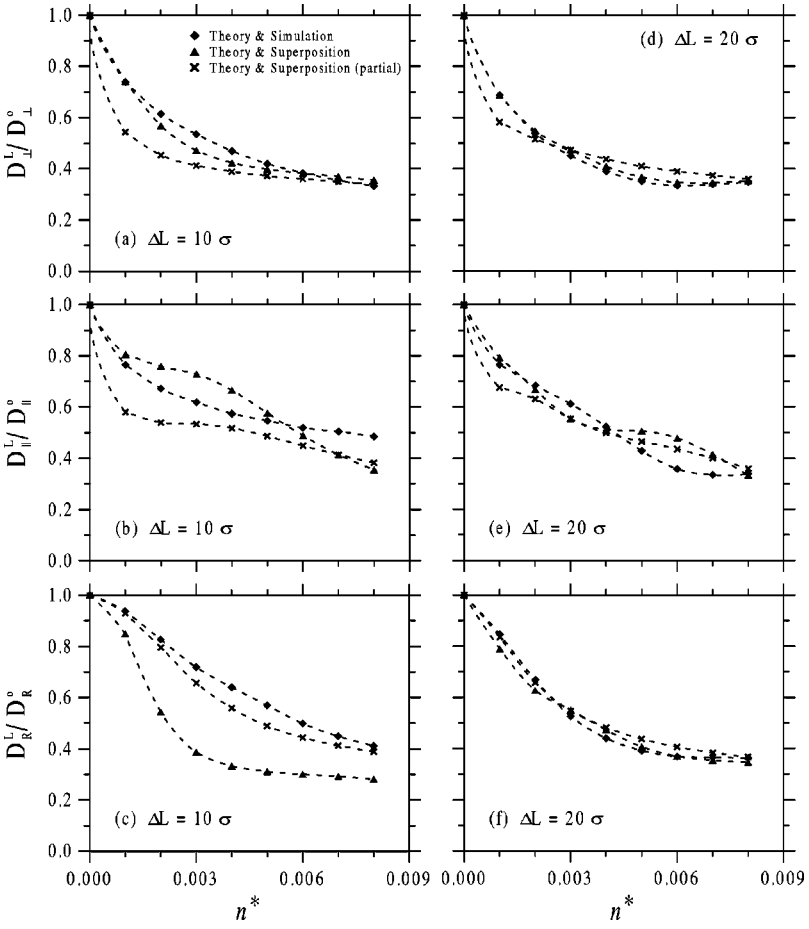

FIG. 4. Comparison between the long-time tracer-diffusion coeficients from the GLE approach with exact (diamonds) and approximate (triangles: full superposition; crosses: partial superposition) input for $n^{eq}(\mathbf{k})$.

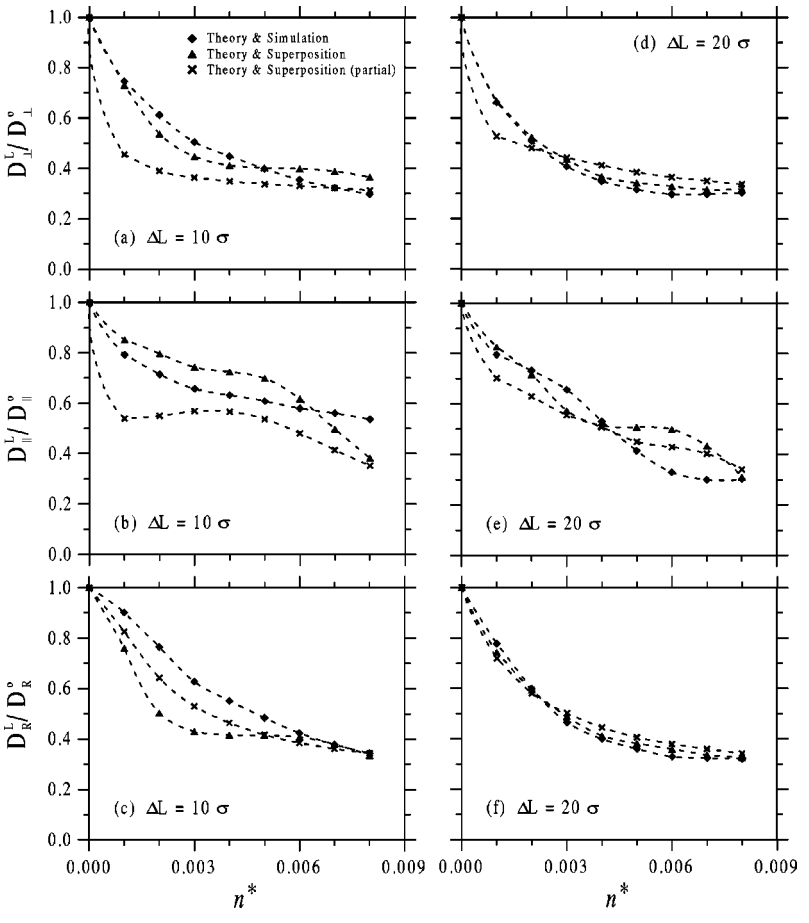

FIG. 5. Same as Fig. 4, but for a trimer ($N_T = 3$).

coeffiecients D_R^L, $D_\perp^L$, and $D_\parallel^L$ of a nonspherical tracer particle that interacts with the spherical particles of a supporting colloidal suspension. These long-time diffusion coefficients were obtained from the extrapolation to $t\to\infty$ of the corresponding time-dependent diffusion coefficient. The data thus obtained were employed as a reference to compare the predictions of an approximate theory derived within the generalized Langevin equation formalism. This theory expresses D_α^L in terms of the purely static structural properties $H(\mathbf{k})$ and $S(k)$, and is based on two major dynamic approximations, whose accuracy we wanted to assess.

In order to do that, in Sec. II we presented the theoretical results for D_α^L obtained using the exact (i.e., simulated) values for the static inputs $H(\mathbf{k})$ and $S(k)$. This allowed us not to introduce additional approximations, so as to see only the effect of the so-called homogeneity and short-time approximations involved in the derivation of Eq. (2.5). Comparing the results thus obtained with the computer simulation data for D_α^L led us to the general conclusion that the theoretical values of D_α^L generally understimate the effects of the direct interactions, to a similar extent as observed before for spherical tracer particles. Other than this systematic quantitative disagreement, we can observe overall a quite good agreement with the simulation data, particularly with regard to the qualitative dependence of $D_\alpha^L(n)$ on the concentration of spheres. This was particularly clear, for example, in the sign of the initial curvature of $D_\alpha^L(n)$, as illustrated in Figs. 2 and 3 by the quadratic expansion of the theoretical expression for $D_\alpha^L(n)$.

All these conclusions refer to the approximate GLE theoretical results obtained using the exact static inputs $H(\mathbf{k})$ and $S(k)$. In Sec. III we also explored the quality of the approximate results obtained from the same GLE expression for D_α^L, but when, instead of the exact $H(\mathbf{k})$, we employed some form of approximation for this static input. We considered two approximations for $H(\mathbf{k})$, namely, the full (Kirkwood) supperposition approximation and what we called the partial superposition approximation. We found that the partial supperposition approximation (for the particular case $\Delta L = 10\sigma$) gave better results for systems with intermediate and high concentrations of spheres. This is, of course, the simplest way to approximate the function $H(\mathbf{r})$. However, for systems with $\Delta L = 20\sigma$, both approximations (the total and the partial superposition approximation) gave results similar to those of the theory with exact inputs.

In summary, the results in this paper showed that the GLE theory of rotational and traslational diffusion of nonspherical particles provides a useful and accurate description of the experimental (i.e., simulated) behavior of the simple model system considered in this work. The comparisons presented in this paper, in addition, will be useful in the process of applying the GLE theory to more realistic systems and conditions.

ACKNOWLEDGMENTS

This work was supported by the Consejo Nacional de Ciencia y Tecnología (CONACyT, México) through Grant No. G295889E and financial support for F.J.G.R. M.M.N. also acknowledges the support of the Programa de Simulación Molecular del Instituto Mexicano del Petróleo (IMP, México), and the National Science Foundation (Grant No. PHY94-07194), and the kind hospitality of the Institute of Theoretical Physics of the University of California at Santa Barbara.

[1] B. U. Felderhof and R. B. Jones, Faraday Discuss. Chem. Soc. **76**, 179 (1983).

[2] P. Pusey, in *Liquids, Freezing and Glass Transition*, edited by J. P. Hansen, D. Levesque, and J. Zinn-Justin (Elsevier, Amsterdam, 1991), Chap. 10.

[3] *Colloid Physics*, edited by G. Nägele, B. D'Aguanno, and A. Z. Akcasu, Physica A **235**, 1 (1997).

[4] J. McConnell, *Rotational Brownian Motion and Dielectric Theory* (Academic Press, London, 1980).

[5] M. Medina-Noyola, Faraday Discuss. Chem. Soc. **83**, 21 (1987); A. Viscarra-Rendón, M. Medina-Noyola, and R. Klein, Chem. Phys. Lett. **173**, 397 (1990).

[6] M. Hernández-Contreras and M. Medina-Noyola, Phys. Rev. E **53**, R4306 (1996); **54**, 6573 (1996); **54**, 6586 (1996).

[7] H. Aranda-Espinoza, M. Carbajal-Tinoco, E. Urrutia-Bañuelos, J. L. Arauz-Lara, and M. Medina-Noyola, J. Chem. Phys. **101**, 10 925 (1994); H. Aranda-Espinoza, M. Medina-Noyola, and J. L. Arauz-Lara, *ibid.* **99**, 5462 (1993).

[8] F. de J. Guevara-Rodríguez and M. Medina-Noyola, J. Chem. Phys. **111**, 1049 (1999).

[9] F. de J. Guevara-Rodríguez and M. Medina-Noyola, J. Chem. Phys. **111**, 1060 (1999).

[10] H. Löwen, J. Phys. Condens. Matter **4**, 10 105 (1992); **5**, 2649 (1993); Phys. Rev. E **53**, R29 (1996).

[11] J. G. Kirkwood, J. Chem. Phys. **3**, 300 (1935).

[12] F. de J. Guevara-Rodríguez and M. Medina-Noyola, Mol. Phys. **95**, 621 (1998).